Compact Large-Displacement Model for a Capacitive Accelerometer

Timo Veijola*, Heikki Kuisma**, and Juha Lahdenperä**

* Helsinki University of Technology, Circuit Theory Laboratory,
Department of Electrical and Communications Engineering,
P.O.Box 3000, FIN-02015 HUT, Finland, timo@aplac.hut.fi
** VTI Hamlin, P.O.Box 27, FIN-01621 Vantaa, Finland.

ABSTRACT

A compact large-displacement model for a gas damped capacitive accelerometer is presented. The gas-film model has been derived from the modified nonlinear Reynolds equation, where the influence of the gas rarefaction is included. The error due to the simplifications in the simple damping model has been compared with those of a finite-difference model. The compact model is constructed of electrical equivalent-circuit blocks consisting of nonlinear controlled current and charge sources. The measured capacitance-voltage characteristics and large-displacement transient responses of an accelerometer are compared with simulation results. The finite element comparisons and the measurements show that the compact model has sufficient accuracy even if the gap displacement is as large as 90 % of the static gap separation.

Keywords: Electrical equivalencies, gas-film damping, squeezed-film damping, accelerometer model, macro model, large-displacement model.

INTRODUCTION

Accelerometers are usually designed to operate in the linear small-displacement region. In modelling their dynamic operation, the use of the linearized Reynolds [1] equation accounting for the effective viscosity is justified in the gas-film damping model. However, in many cases the relative change in the air-gap is large resulting also in large variations in the gas pressure, invalidating the use of the linearized gas-film model. In these cases, the modified nonlinear Reynolds equation with the pressure- and displacement-dependent flow rate coefficient must be applied [2].

In addition to the gas-film forces, there are several nonlinear phenomena that must be considered in an accurate large-displacement accelerometer model. The necessary simplification for a simple, compact simulation model is that the higher-order resonance modes of the proof mass are ignored.

A complete accelerometer model can be constructed using electrical equivalent-circuit blocks, as we demonstrated in [3]. In this paper, first, a few improvements in the model are presented: the nonlinear gas-film damping model is revised and validated with a comparison to a more accurate finite-difference (FD) model [4]. Also, a new simple model for the mass collision with the isolating stubs is presented. Finally, the measured capacitance-voltage characteristics and large-displacement transient responses of an accelerometer are compared with simulation results.

The gas-film model presented in [5] has been verified by comparing its response with a full 3D numerical solution of the Navier-Stokes equations [6]. Other large-displacement accelerometer simulations have been presented in [7], and a mathematical model for an accelerometer has been published in [8].

ACCELEROMETER STRUCTURE

The structure of a bulk micromachined accelerometer is shown in Fig. 1. The seismic mass is nonsymmetrically supported by a cantilever beam. The change in the displacement of the two symmetric air gaps is detected capacitively. The large-displacement motion of the mass is limited with small isolating stubs, and the sensor motion is damped by gas in the air gaps.

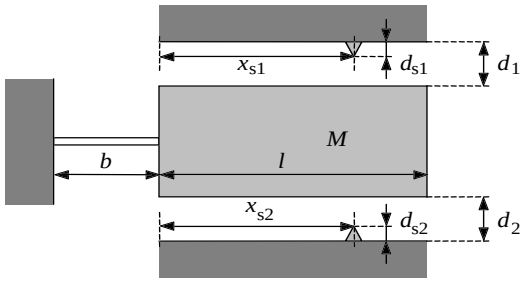

Figure 1: The structure of a bulk micromachined accelerometer manufactured by VTI Hamlin. The gap dimensions are not drawn to scale.

An accurate dynamic model describing the operation of the sensor is complicated: due to the asymmetrical structure the gap is not uniform along the surface, especially at large relative displacements. In that case no analytic gas-film model cannot be found, even if the pressure changes are assumed small compared to the ambient pressure. Large displacements relative to the gap separation also couple the motion of the fundamental resonance mode to an additional twisting mode. The

motion coupling between the modes is very strong when the mass hits the stubs that limit the displacement.

GAS-FILM MODEL

Modified Reynolds equation

A nonlinear partial differential equation, the Reynolds equation [2], is used in lubrication theory to determine the behaviour of a thin fluid film between two moving surfaces. When the surfaces do not move in the x- or y-directions, the modified Reynolds equation is

$$\frac{\partial}{\partial x}\left[\rho h^3 Q_{\rm pr}\frac{\partial p}{\partial x}\right]+\frac{\partial}{\partial y}\left[\rho h^3 Q_{\rm pr}\frac{\partial p}{\partial y}\right]=12\eta\frac{\partial(\rho h)}{\partial t}, \qquad (1)$$

where ρp^{-n} is a constant, and gas density ρ, pressure p, and the gap separation h are functions of time t and position $(x,\, y)$. η is the viscosity of the gas and $Q_{\rm pr}$ is the relative flow rate coefficient. In spite of the large-displacement conditions, the heat generation in the gas is very small. Thus, an isothermal process is assumed ($n=1$), and density ρ can be replaced with pressure p.

The relative flow rate coefficient $Q_{\rm pr}$ is needed in modelling the rarefied gas flow in narrow gaps. It is a function of the Knudsen number $K_{\rm n}$, that is the ratio between the mean free path of the gas molecules and the gap separation. $K_{\rm n}=\lambda/h=\lambda_0 P_0/p/h$, where λ_0 is the mean free path of the gas at pressure P_0. The relative flow rate coefficient is derived from the linearized Boltzmann equation [9]. A simple approximation for the relative flow rate coefficient is [5]

$$Q_{\rm pr}=1+9.638(K_{\rm n})^{1.159}. \qquad (2)$$

A better approximation including the impact of the gas-surface interaction is given in [9].

Gas-film model for parallel surfaces

When the surfaces move perpendicularly, the gap separation h is not a function of x or y positions. Since p is a function of position and time, and $Q_{\rm pr}$ is generally a function of p and h, the partial derivation of Eq. (1) yields

$$\frac{h^3}{12\eta}\left\{pQ_{\rm pr}\left[\frac{\partial^2 p}{\partial x^2}+\frac{\partial^2 p}{\partial y^2}\right]\right. \qquad (3)$$
$$\left.+\left(Q_{\rm pr}+p\frac{\partial Q_{\rm pr}}{\partial p}\right)\left[\left(\frac{\partial p}{\partial x}\right)^2+\left(\frac{\partial p}{\partial y}\right)^2\right]\right\}=\frac{\partial(ph)}{\partial t}.$$

If it is assumed that the dynamic pressure change Δp is small compared to the ambient pressure $P_{\rm a}$ ($p=P_{\rm a}+\Delta p$), Eq. (3) reduces further to

$$\frac{h^2 Q_{\rm pr}}{12\eta}\left[\frac{\partial^2\Delta p}{\partial x^2}+\frac{\partial^2\Delta p}{\partial y^2}\right]=\frac{1}{P_{\rm a}}\frac{\partial(\Delta p)}{\partial t}+\frac{1}{h}\frac{\partial h}{\partial t}. \qquad (4)$$

If now small-displacement conditions are assumed, that is, $\partial h/\partial t$ is replaced with $\partial\Delta p/\partial t$, h is replaced with d and $Q_{\rm pr}$ is assumed constant, an analytic solution for the force acting on rectangular surfaces can be found [1].

Gas-film equivalent-circuit model

After applying the electrical equivalencies for mechanical quantities (velocity is equivalent to voltage $u_{\rm v}$), the gas-film force acting on the surfaces can be described by an electrical equivalent-circuit [5], see Fig. 2. Each RL-section in the circuit models one Fourier-series term of the force. Since the dynamic pressure distribution on the surface is almost sinusoidal, a few sections are sufficient for a relatively good approximation. The compo-

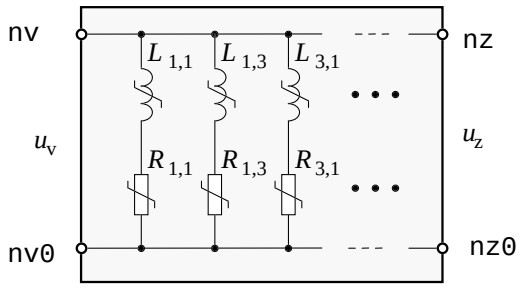

Figure 2: The gas-film damping model for rectangular geometry. Nonlinear inductances and resistances are controlled by the displacement z.

nent values in the circuit are

$$R_{m,n} = (mn)^2\left(\frac{m^2}{w^2}+\frac{n^2}{l^2}\right)\frac{\pi^6 h^3 Q_{\rm pr}(h,P_{\rm a})}{768 l w\eta}, \qquad (5)$$

$$L_{m,n} = (mn)^2\frac{\pi^4 h}{64 l w P_{\rm a}}, \qquad (6)$$

where m and n are odd integers, and w and l are the width and length of the surface, respectively. The large-displacement approximation was made by replacing the static gap separation d in the linear solution with the displacement h and using displacement-dependent $Q_{\rm pr}$ in Eqs. (5) - (6). The component values now depend on an external displacement voltage $u_{\rm z}$, since $h=d\pm a u_{\rm z}$, where the positive and negative signs are for the lower and upper air gaps, respectively. a is a displacement scaling constant [m/V].

It is still assumed in Eqs. (5) - (6) that the pressure variation is small compared to the ambient pressure and that the Knudsen number does not depend on Δp. However, for an accurate model it is essential that the relative flow rate coefficient $Q_{\rm pr}$ is a function of the large-displacement gap separation h. This was not realized in the previous models [3], [5], [6]. For small-displacement cases $Q_{\rm pr}$ can be considered constant and the term effective viscosity $\eta_{\rm eff}=\eta/Q_{\rm pr}$ is then usable [5].

Comparison with the FD model

The accuracy of the compact model is compared with a model that realizes Eq. (1) with a finite-difference

mesh [4]. Influence of the mesh size on the error is also studied. A step acceleration excitation is applied to the accelerometer model. The parameters of the model contain the dimensions of a device manufactured by VTI Hamlin. However, motion normal to the surfaces is assumed here ($b = \infty$).

Table 1 shows maximum errors relative to the final gap separation at three excitation levels resulting in step displacements of $0.5\,d$, $0.7\,d$, and $0.9\,d$. The FD solution with a 50×50 mesh was used as a reference [4]. Simulated step responses of the reference FD model and the compact model (3 sections) are shown in Fig. 3.

From Table 1 it can be seen that a displacement-independent relative flow rate coefficient $Q_{\rm pr}(d, P_{\rm a})$ yields errors of the same order as the linear model. However, the use of constant $Q_{\rm pr}$ underestimates the displacement, whereas the linear model overestimates it.

Displacement step	$0.5\,d$	$0.7\,d$	$0.9\,d$
Linear model	12	31	69
Compact model, constant $Q_{\rm pr}$	8.8	25	69
Compact model, 1 section	3.3	5.1	8.2
Compact model, 3 sections	0.76	1.4	2.6
Compact model, 5 sections	0.46	1.0	2.0
FD model, 5x5 mesh	4.0	5.9	8.3
FD model, 10x10 mesh	1.2	1.7	2.4
FD model, 20x20 mesh	0.28	0.42	0.59

Table 1: Maximum displacement errors in percent relative to the final gap separation of three different gas-film models.

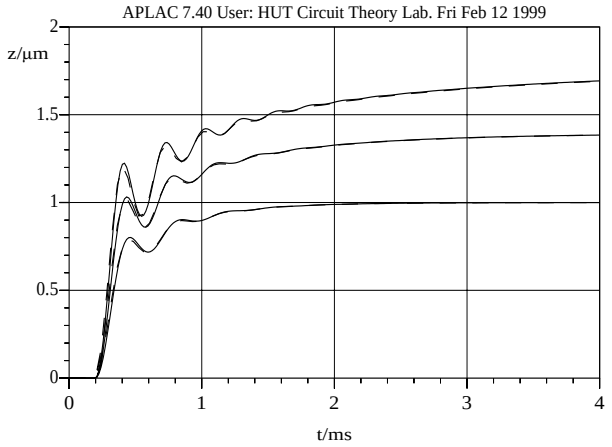

Figure 3: Accelerometer step responses with three excitation levels simulated with the FD model (– – –) and the compact model (——). Gap separation is $2\,\mu$m and the pressure is 300 Pa.

The influence of the tilting motion on the gap capacitance is studied in Table 2. The response of the FD model (50×50 mesh), that is again used as a reference, includes the impact of the nonsymmetric support of the mass. The cantilever beam length b (effective bending length) varies between the surface length l and $l/4$.

Mass tip step displ.	$\approx 0\,d$	$0.5\,d$	$0.7\,d$	$0.9\,d$
$b = l$	1.4	2.6	3.5	5.9
$b = l/2$	2.1	4.1	5.6	9.1
$b = l/4$	3.1	5.9	7.9	12

Table 2: Maximum compact model (three sections) capacitance errors in percent relative to the capacitance change caused by a stepwise excitation.

ACCELEROMETER MODEL

A complete simulation model for an accelerometer is constructed with the gas-film model presented above, and electrical equivalent-circuit blocks, as documented in [3]. The blocks include the mass-spring system block, an electromechanical transducer block for tilting surfaces (capacitance and electrostatic force), and an additional block to model the collision of the mass to the limiter stub. The model has been implemented in the circuit simulation and design tool APLAC [10].

Displacement limiter stubs

When the displacement of the mass is large it hits the limiter stubs. Due to the mass inertia, or due to an electrostatic force, the mass will tilt around the stub still increasing the capacitance. However, the actual mass movement is not modelled here, and the increase of the capacitance is included as a finite elasticity of the stub. When applying the electrical equivalencies used in the implementation, the exponential stub force is modelled with a nonlinear controlled current source $i_{\rm s}$:

$$i_{\rm s} = F_{\rm s}(e^{\kappa z/z_{\rm max}} - 1) + G_{\rm s}(e^{\kappa z/z_{\rm max}} - 1)u_{\rm v}, \qquad (7)$$

where $F_{\rm S0}$ and $G_{\rm S0}$ are the force and viscosity constants, κ is the stub 'hardness' and $z_{\rm max}$ is the maximum displacement that are extracted from measurements.

EXPERIMENTAL

Capacitance-voltage characteristics of an accelerometer are measured with a slow voltage ramp from $0\,V$ to $10\,V$, and from 10 V to -10 V and back to 0 V. All model parameters, except the gas-film parameters, are extracted by fitting the model response to the measured characteristics, see Fig. 4.

The capacitance response of the same device is measured using pulsed actuating voltages. Figure 5 shows six measured transient responses together with simulation results with the FD model (50×50 mesh) and the compact model (3 section for both air-gaps). In three of them a snap-in phenomenon occurs, and in two cases the mass displacement is smaller. The device response

is slow because of the relatively large gas pressure (≈ 30 kPa) inside the accelerometer. The pressure parameter in both models has been determined by fitting the responses of the FD model to the measured responses.

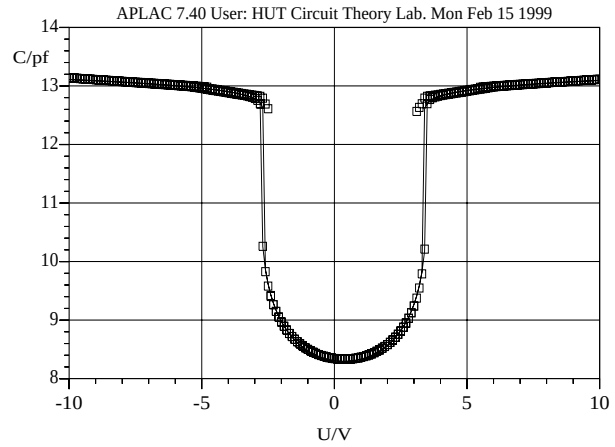

Figure 4: Measured (□) and simulated (——) accelerometer capacitance-voltage characteristics. The stubs limit the displacement at the tip of the mass to about 60 % of the gap separation (2 μm), resulting in a maximum capacitance of about 13 pF ($b/l \approx 0.3$). Curve fitting techniques were used here.

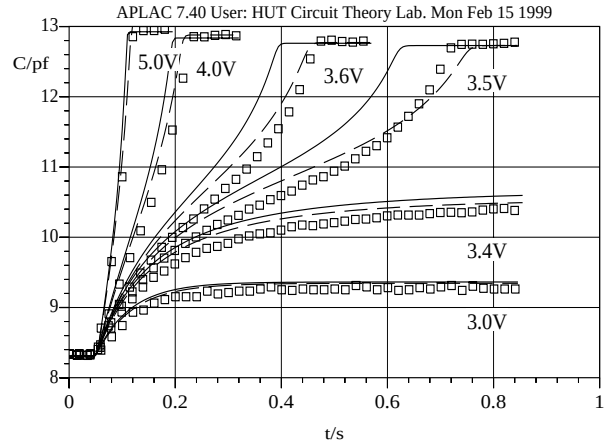

Figure 5: Measured (□) accelerometer capacitance responses for six electrostatic step-voltage excitations and simulated accelerometer model responses using the compact gas-film model (——) and the FD model (– – –).

CONCLUSIONS

A compact large-displacement model for a capacitive accelerometer including nonlinear gas-film forces in the air-gap was presented. It was shown that a simple gas-film model for parallel surfaces with an error less than 3 % is usable for displacements up to 90 % of the gap separation. Comparative simulations with a more accurate finite-difference model for parallel surfaces show that the element count is reduced from 100 to 3 without any loss in the accuracy. The model is usable also in modelling the gas-film forces between tilting, rectangular surfaces, as was shown in the comparison with measurements of an accelerometer with nonsymmetric mass support.

Since the pressure distribution can be assumed to be independent of the gap separation, a similar compact model for more complicated boundary conditions for the gas flow can be derived. In the small-displacement conditions, the influence of the tilting motion could be modelled more accurately with additional RL-sections. However, the improvement achieved in the large-displacement conditions would be insignificant.

REFERENCES

[1] J. J. Blech, "On isothermal squeeze films," *Journal of Lubrication Technology*, vol. 105, pp. 615–620, Oct. 1983.

[2] S. Fukui and R. Kaneko, "A database for interpolation of Poiseuille flow rates for high Knudsen number lubrication problems," *Journal of Tribology, Trans. ASME*, vol. 112, pp. 78–83, Jan. 1990.

[3] T. Veijola, H. Kuisma, and J. Lahdenperä in *Proceedings of MSM'98*, (Santa Clara), pp. 245–250, Apr. 1998.

[4] T. Veijola, "Finite-difference large-displacement gas-film model," in *Proceedings of Transducers'99*, (Sendai), June 1999. Manuscript in review.

[5] T. Veijola, H. Kuisma, J. Lahdenperä, and T. Ryhänen, "Equivalent circuit model of the squeezed gas film in a silicon accelerometer," *Sensors and Actuators A*, vol. 48, pp. 239–248, 1995.

[6] M. Turowski, Z. Chen, and A. Przekwas, "Squeeze film behavior in MEMS for large amplitude motion - 3D simulations and nonlinear circuit/behavioral models," in *IEEE/VIUF International Workshop on Behavioral Modeling and Simulation*, (Orlando), Oct. 1998.

[7] Y. J. Yang, M. A. Gretillat, and S. D. Senturia, "Effect of air damping on the dynamics of nonuniform deformations of microstructures," in *Proceedings of Transducers'97*, (Chicago), pp. 1093–1096, June 1997.

[8] C. P. Lewis, M. Kraft, and T. G. Hesketh, "Mathematical model for a micromachined accelerometer," *Trans. Inst. MC*, vol. 18, no. 2, pp. 92–98, 1996.

[9] T. Veijola, H. Kuisma, and J. Lahdenperä, "The influence of gas-surface interaction on gas film damping in a silicon accelerometer," *Sensors and Actuators A*, vol. 66, pp. 83–92, 1998.

[10] M. Valtonen *et al.*, *APLAC*. Helsinki University of Technology and Nokia Research Center, 7.1 Reference Manual and 7.1 User's Manual, Otaniemi, Oct. 1997. http://www.aplac.hut.fi/aplac.